Progress In Electromagnetics Research, Vol. 144, 291–302, 2014

Performance Enhancement of Target Recognition Using Feature Vector Fusion of Monostatic and Bistatic Radar

Seung-Jae Lee[1], In-Sik Choi[1, *], Byung-Lae Cho[2], Edward J. Rothwell[3], and Andrew K. Temme[3]

Abstract—This paper proposes a fusion technique of feature vectors that improves the performance of radar target recognition. The proposed method utilizes more information than simple monostatic or bistatic (single receiver) algorithms by combining extracted feature vectors from multiple (two or three) receivers. In order to verify the performance of the proposed method, we use the calculated monostatic and bistatic RCS of three full-scale aircraft and the measured monotatic and bistatic RCS of four scale-model targets. The scattering centers are extracted using one-dimensional FFT-based CLEAN and then used as feature vectors for a neural network classifier. The results show that our method has better performance than algorithms that solely use monostatic or bistatic data.

1. INTRODUCTION

Traditional radars are monostatic, meaning that the transmitter and receiver are located at the same position. Thus, most previous studies on radar target recognition assume a monostatic arrangement. The recognition algorithms generally involve feature vectors consisting of scattering center information from the early-time response or resonant frequency information from the late-time response [1–3]. Scattering centers are those points on the target associated with strong scattered fields while natural resonant frequencies arise from global interactions and are related to the physical size of the target. Scattering center data tend to be strongly resistant to noise with relatively high energy [1, 4], and are most useful when describing target characteristics at higher frequencies than resonance data. For these reasons, scattering centers are used as a feature vector for target recognition in this paper.

Many recent studies have considered using a monostatic radar with scattering centers as feature vectors. The authors in [4] conducted a target classification experiment using the feature vectors extracted in an efficient way that takes advantages of both the model-based technique and the FFT-based CLEAN algorithm. In [5], a study compared the FFT-based CLEAN algorithm, TLS (total least squares)-Prony method, and the EP (Evolutionary Programming)-based CLEAN technique. In [6], the scattering centers were extracted and target recognition performance was compared among the IFFT (Inverse fast Fourier Transform), TLS-Prony, GEESE (generalised eigenvalues utilising signal subspace eigenvectors), and MP (matrix-pencil) methods.

The development of radar cross section (RCS) reducing technology has produced a wealth of low-RCS radar targets. In response, the radar community has turned to bistatic radars whose transmitter and receiver are placed in different positions as a means to enhance detection [7–10]. Low-RCS targets are designed to minimize the backscattering signal using radar absorbing materials (RAM), and thus do not produce a strong signal to monostatic radars [11]. This explains to the improved effectiveness of bistatic radar compared to monostatic radar [10]. Unfortunately, little research has been undertaken to

Received 31 October 2013, Accepted 22 January 2014, Scheduled 29 January 2014

* Corresponding author: In-Sik Choi (recog@hannam.ac.kr).

[1] Department of Electronic Engineering, Hannam University, Daejeon, Republic of Korea. [2] Defense Advanced R&D Institute, Agency for Defense Development (ADD), Daejeon, Republic of Korea. [3] Department of Electrical and Computer Engineering, Michigan State University, East Lansing, MI 48824, USA.

study target recognition using bistatic radar. One such study is [12], which compares the performance of monostatic and bistatic radar target classification schemes using the computed bistatic RCS (BRCS) of simple wire targets and time-frequency analysis for target feature extraction.

The studies mentioned above each used a feature vector extracted from either the monostatic radar return or from the bistatic radar return in target classification experiments. The present paper proposes a feature vector fusion technique that combines the feature vectors extracted from both monostatic and bistatic radar returns with an aim to enhance the performance of target recognition.

Both numerical and experimental data is used to explore the effectiveness of the proposed vector fusion technique. First the monostatic RCS (MRCS) and the BRCS of full-scale 3-D models was calculated at various aspect angles using FEKO, a commercial EM solver. Then measurements of four scale model targets were made using the scattering range at Michigan State University. The 1-D FFT-based CLEAN algorithm, which is known to be strongly resistant to noise, was used to extract the scattering centers of the targets from both computed and measured data, and the feature vectors of the targets thus obtained were used as inputs to a neural network classifier. We used the MLP (multilayer perceptron) classifier, which is one of the standard classifiers, because the classification accuracy of these classifiers is the same [13].

Target recognition performance was investigated for three cases. In each case a transmitter position was established and one or more receivers were placed in monostatic or bistatic positions. The first case uses a single receiver (monostatic or bistatic). The second case assumes two receivers, one monostatic and one bistatic. The third case uses three receivers, one monostatic and two bistatic. Experiments show that combining multiple feature vectors, as in the third case, produces the best classifier performance.

2. PROPOSED METHOD

2.1. Feature Extraction Using FFT-Based CLEAN

There are various methods for obtaining one-dimensional (1-D) scattering centers, including using FFT-based CLEAN [4, 14, 15], an EP-based method [1, 5], and a model-based method such as Prony's method [16]. Model-based methods have high resolution characteristics, but are very sensitive to random noise and require an accurate estimation of the number of scattering centers present in the data, as determined by using some information-based criterion (typically with a large computational cost) [16]. EP-based CLEAN was developed to overcome these difficulties. It has demonstrated both high resolution and robustness to model order. However, it is computationally much more costly than Prony's method or FFT-based CLEAN [1, 5]. FFT-based CLEAN is a good candidate for 1-D scattering center extraction even though it has lower resolution, since it has a strong resistance to random noise and is computationally fast. In this paper, the test data is mixed with random noise, so an algorithm is required that is robust to noise. Therefore, the FFT-based CLEAN algorithm was adopted to extract the scattering centers. Since the CLEAN algorithm assumes an undamped exponential model, an undamped exponential model is used in this study. The undamped exponential model of the scattered signal in the high-frequency region is as follows [4, 5]:

$$E\left(f_q\right) = \sum\nolimits_{m=1}^{M} a_m \exp\left(-\frac{j4\pi f_q R_m}{c}\right), \quad q = 1, \ldots, Q \tag{1}$$

where M is the number of scattering centers, f_q the frequency at sample q, Q the number of frequency samples, R_m the location of mth scattering center, a_m the associated amplitude, and c the speed of light.

The FFT-based CLEAN algorithm is a technique to extract scattering centers according to signal energy. The details of the algorithm proceed as follows.

Step 1. (Initialization) Set $m = 1$ where m is the index of iteration to extract the mth scattering center and define the stepped-frequency measured data as $E_m(f_q)$ for $q = 1, \ldots, Q$.

Step 2. (Range profile generation) Obtain the range profile using inverse fast Fourier transform (IFFT) as follows:

$$rp_m\left(r_q\right) = abs\left[F^{-1}\left\{E_m\left(f_q\right)\right\}\right] \tag{2}$$

where r_q is the qth range bin defined as $(q-1) \times \Delta R$ with ΔR the range resolution $(\frac{c}{2BW})$ and abs means the absolute values.

Step 3. (Parameter extraction) After obtaining the range profile, the a_m and R_m are extracted using the peak search method. The global maximum location $r_{q\max}$ is determined as the location of mth scattering center (R_m) and the complex amplitude at that point ($r_{q\max}$) is determined as a_m.

Step 4. (Elimination of extracted signal) After the a_m and R_m are found at the Step 3, the point spread function can be obtained using IFFT as

$$psf_m(r_q) = abs\left[F^{-1}\left\{a_m \exp\left(-\frac{j4\pi f_q R_m}{c}\right)\right\}\right] \tag{3}$$

The point spread function is sinc function, since we use the rectangular window in Eq. (3). Then, the point spread function $psf_m(r_q)$ is subtracted from the range profile $rp_m(r_q)$ to give $rp_{m+1}(r_q)$:

$$rp_{m+1}(r_q) = rp_m(r_q) - psf_m(r_q), \quad q = 1, \ldots, Q \tag{4}$$

Step 5. (Termination check) Let $m = m + 1$. Return to Step 3, unless the desired M scattering centers are extracted. In this paper, it is assumed that M is known and fixed for all targets and aspect angles. In neural network-based target recognition, the feature vectors must have the same dimension. Therefore, M is fixed and the FFT-based CLEAN process is terminated when the iteration index m reaches the predetermined value M.

After the extraction of M scattering centers, their ranges are assorted in ascending order. Next, the shift-invariant feature vector $\mathbf{f}$, which is used as the neural network input, is obtained as follows:

$$\mathbf{f} = [|a_1|, |a_2|, |a_3|, \ldots, |a_M|, d_{12}, d_{13}, d_{14}, \ldots, d_{1M}] \tag{5}$$

where $|a_i|$, for $i = 1, 2, \ldots, M$, is the absolute value of the complex valued amplitude a_i sorted in descending order, and d_{1j}, $j = 2, \ldots, M$, is the relative distance between d_1 and d_j sorted in ascending order. Figure 1 shows an example of the 11 dimensional feature vector when the number of scattering centers $M = 6$.

2.2. Feature Vector Fusion

Figure 2 illustrates an overall block diagram of the feature vector fusion technique, which this paper proposes for improving the target recognition performance. Rx1 is the monostatic receiver and Rx2

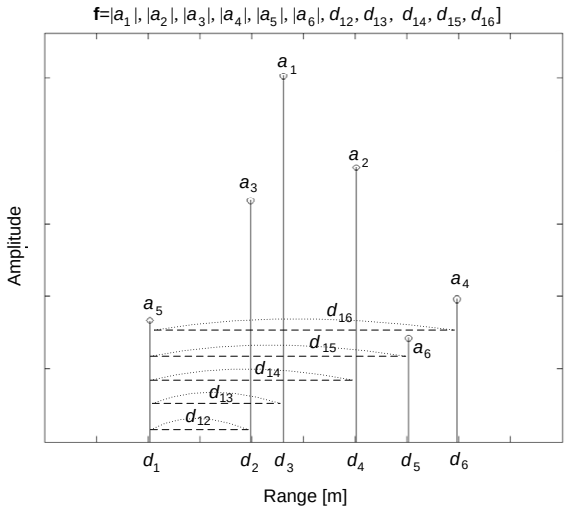

Figure 1. Example of feature vector extraction, $M = 6$.

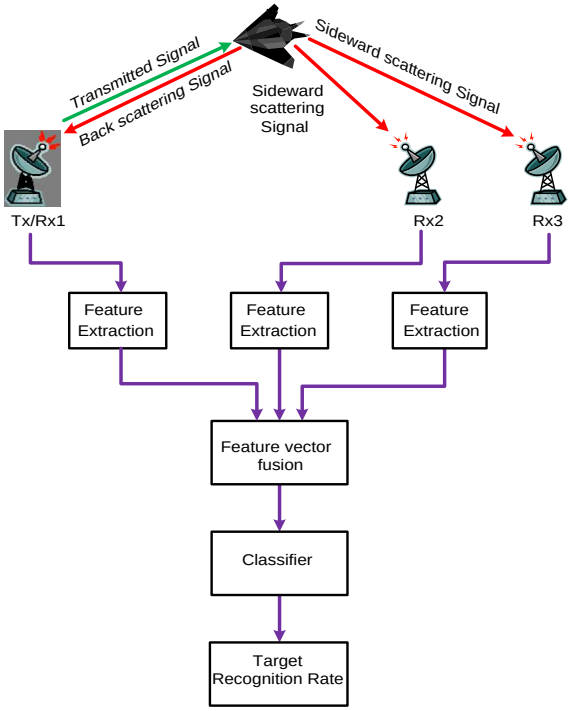

Figure 2. Block diagram for feature vector fusion.

and Rx3 are the bistatic receivers. Rx1 receives the backscatter signal of the target and Rx2 and Rx3 receive the signals scattered sideward. For the target recognition experiments, these scattering signals can be obtained by simulation or measurements.

Next, the feature vectors extracted from each of the scattering data received by Rx1, Rx2 and Rx3 using the 1-D FFT-based CLEAN algorithm. These extracted feature vectors are then passed through the fusion stage where those feature vectors extracted from monostatic receiver and bistatic receivers are combined together, providing added information for the classifier.

The feature vector $\mathbf{f}_{c1}$, which results from combining feature vectors extracted from the monostatic receiver and from one bistatic receiver, is defined as

$$\mathbf{f}_{c1} = [\mathbf{f}_{\mathrm{Rx1}},\ \mathbf{f}_{\mathrm{Rx2}}] \tag{6}$$

Here $\mathbf{f}_{\mathrm{Rx1}}$ refers to the feature vector extracted from the monstatic receiver Rx1, and $\mathbf{f}_{\mathrm{Rx2}}$ refers to the feature vector extracted from the bistatic receiver Rx2. Note that $\mathbf{f}_{c1}$ has a dimension of 22, since $\mathbf{f}_{\mathrm{Rx1}}$ and $\mathbf{f}_{\mathrm{Rx2}}$ each have a dimension of 11.

The feature vector $\mathbf{f}_{c2}$, which results from combining feature vectors extracted from monostatic receiver and from the two bistatic receivers, is defined as

$$\mathbf{f}_{c2} = [\mathbf{f}_{\mathrm{Rx1}},\ \mathbf{f}_{\mathrm{Rx2}},\ \mathbf{f}_{\mathrm{Rx3}}] \tag{7}$$

where $\mathbf{f}_{\mathrm{Rx3}}$ is the feature vector extracted from the bistatic receiver Rx3, which is different in position from Rx2. Thus, $\mathbf{f}_{c2}$ has a dimensions of 33. The combined feature vectors, $\mathbf{f}_{c1}$ and $\mathbf{f}_{c2}$, are used as input to the neural network classifier. Finally, a target recognition experiment is conducted and a target recognition rate is obtained.

3. RESULTS

The performance of the proposed algorithm was determined through simulation and measurement. Performance was first investigated using the numerically calculated data from CAD models of three different aircraft targets. Figure 3 shows the targets used in the simulations. The target dimensions are actual scale, as shown in Table 1.

FEKO was then used to calculate the RCS of each target in the frequency range 150–404 MHz with 128 frequency samples and HH polarization. To reduce the computational time, the Physical Optics option was used. The nose of each target was placed at the position (0, 0, 0), and the incident field vector was chosen to lie in the x-y plane (elevation angle of 0°), with the electric field horizontally polarized.

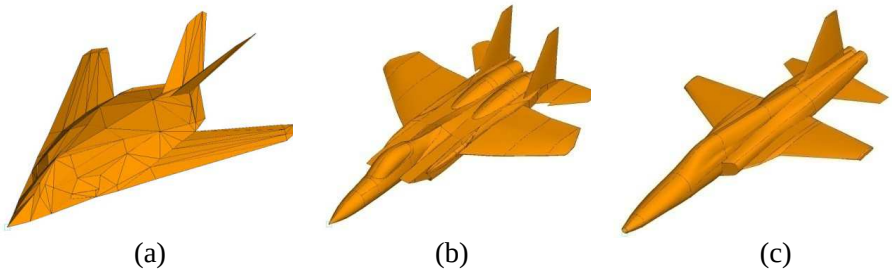

Figure 3. Three 3D CAD models of targets used in the simulation, (a) F-117, (b) F-15, and (c) F-5.

Table 1. Dimensions of three CAD models.

Target	Length [m]	Width [m]
F-117	21	14
F-15	19	13
F-5	14.2	8.2

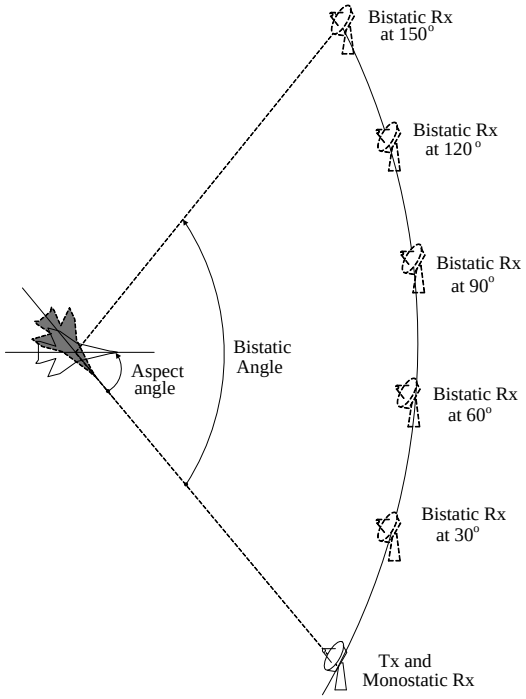

Figure 4. Configuration for monostatic and bistatic RCS calculations.

Figure 4 shows the configuration for the monostatic and bistatic RCS calculation. The transmitter Tx is placed at 0° and the receiver positions are varied from 0° to 150° with a 30° angle interval. At each monostatic and bistatic angle, the targets are also rotated in the x-y plane from 0° to 150° with a 2° aspect angle step.

Next, feature vectors were extracted for each target using 1-D FFT-based CLEAN. Figure 5 and Figure 6 show examples of scattering centers extracted from the monostatic and bistatic (bistatic angle = 30°) RCS, respectively of the F-117 at 0° aspect angle. The extracted 6 scattering centers (labeled o) match well with the peaks of the range profile. The feature vectors described by Eq. (5) have a dimension of 11, which includes the amplitudes of 6 scattering centers and 5 relative distances between the first and the other scattering centers.

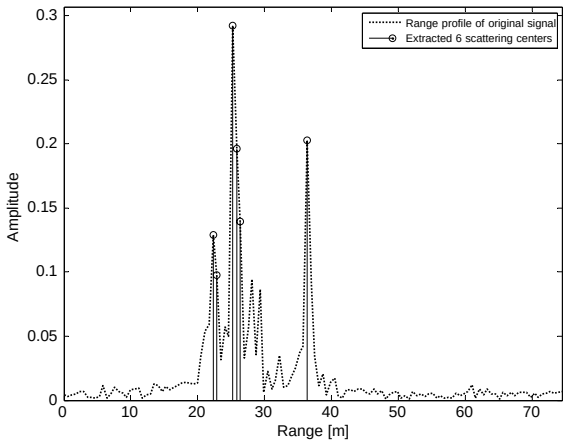

Figure 5. Extracted scattering centers from monostatic RCS of F-117 at aspect angle of 0°, SNR = 20 dB.

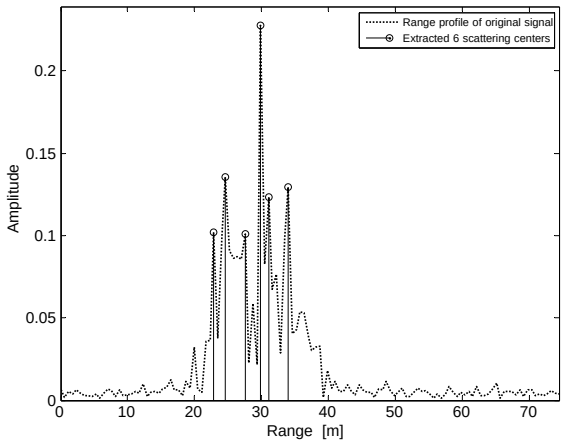

Figure 6. Extracted scattering centers from BRCS (bistatic angle = 30°) of F-117 at aspect angle of 0°, SNR = 20 dB.

The MLP neural network with two hidden layers was then used to perform a target recognition experiment [12, 17]. The MLP neural network configuration is shown in Figure 7. The number of neurons in the first hidden layer was chosen to be twice of the feature vector dimension, and that in the second hidden layer was chosen as the half of that in the first hidden layer. Also, the number of neurons in the output layer is same as the number of targets. To improve the classifier performance, we trained it until the mean square error (MSE) was 10^{-5}.

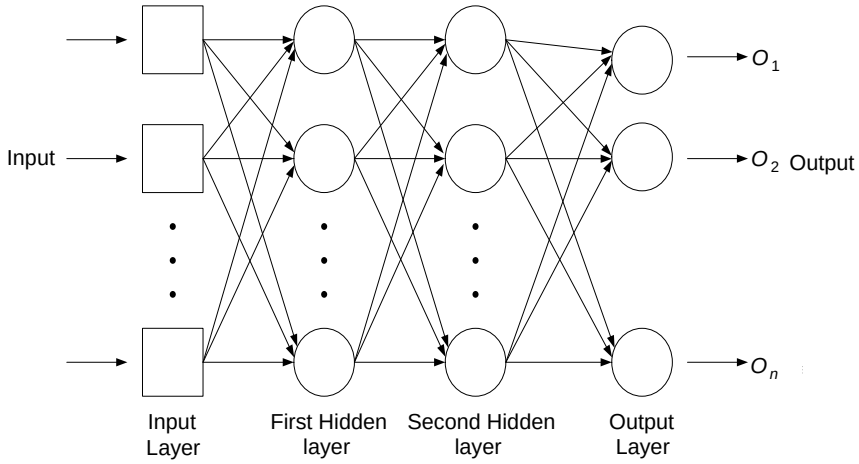

Figure 7. The MLP neural network configuration.

The feature vectors were established at aspect angles over the range 0° to 150° with a 2° step for each target. The noiseless feature sets were used for training. Then, white Gaussian noise at a specified SNR was added to the original signals of all targets. The noisy feature sets at a given SNR are used for testing. Therefore, there are $3 * 76 = 228$ noiseless feature sets for training, and $3 * 76 = 228$ noisy feature sets for testing. The target recognition rate (P_c) is defined as

$$P_c = \frac{\text{total number of correct identifications}}{\text{number of targets} \times \text{number of aspects for testing}} \times 100(\%) \tag{8}$$

Before checking whether or not the proposed feature vector fusion technique improves the target recognition performance, the target recognition experiment was first carried out using only the single feature vector extracted from either the monostatic or bistatic receivers. Figure 8 shows the mean and standard deviation (with bar) of target recognition rates when using the feature vector extracted using only the single receiver. A Monte Carlo analysis was used to establish statistics for the target recognition rate. The mean and standard deviation were computed using only 30 trials, due to the computational expense of each trial. As shown in Figure 8, the target recognition performance is found to be significantly different depending on the position of the receivers, indicating that the position of the transmitter and receivers has a strong effect on the target recognition rate. The best target recognition rate is found to occur at the bistatic angle of 150°.

Next, to establish the performance of the proposed method, the best target recognition rate identified in the above experiment was compared with the target recognition performance in the case where feature vectors were extracted from two receivers (monostatic + one bistatic receiver). As can be seen in Eq. (6), the combined feature vector $\mathbf{f}_{c1}$ has a dimension of 22. Figure 9 shows the results of comparing the target recognition rates for the two cases, fusion and non-fusion. As before, 30 Monte Carlo trials were conducted. According to Figure 9, the target recognition performance of three fusion feature sets (monostatic + bistatic angle = 60°, monostatic + bistatic angle = 90 °, monostatic + bistatic angle = 150°) are better than the best non-fusion feature set (150° bistatic angle). The best performance is found for the fusion of monostatic + bistatic angle = 150°.

Finally, the target recognition performance was examined in the case where feature vectors were extracted from three receivers (monostatic + two bistatic receivers). As can be seen in Eq. (7), the combined feature vector $\mathbf{f}_{c2}$ has a dimension of 33. Table 2 shows the results of comparing target

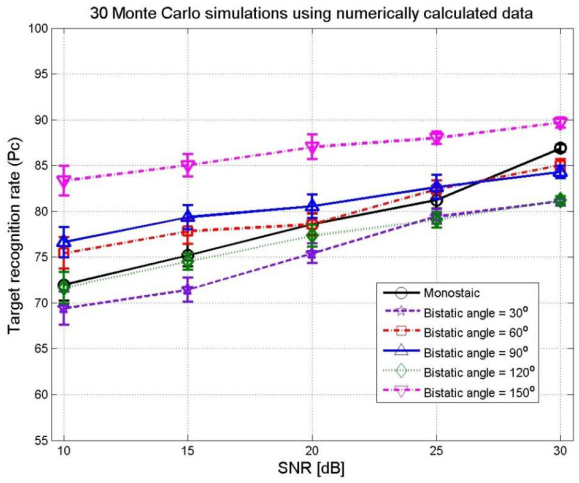

Figure 8. Performance comparison of radar target recognition using a single feature vector for calculated data.

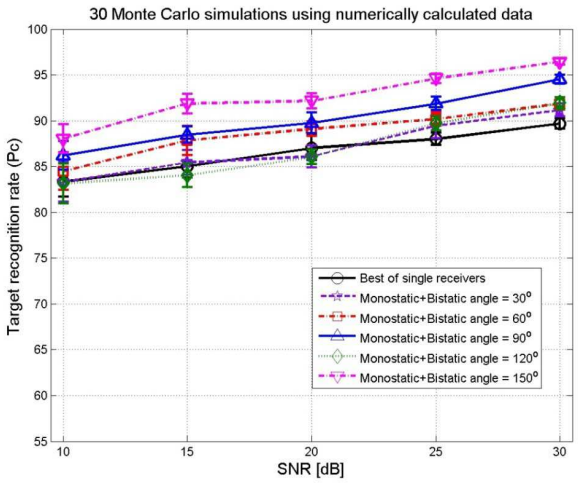

Figure 9. Performance comparison of radar target recognition using two feature vector fusion (monostatic + one bistatic receiver) for calculated data.

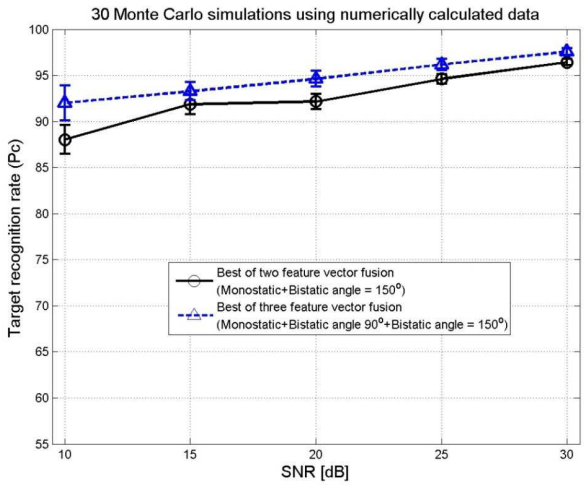

Figure 10. Performance comparison of radar target recognition for the best feature vector fusions of calculated data.

recognition rates for various $\mathbf{f}_{c2}$. The best performance is found for the fusion of monostatic + bistatic angle = 90° + bistatic angle = 150°. To compare the performance of $\mathbf{f}_{c1}$ and $\mathbf{f}_{c2}$, the best results were examined. Figure 10 shows that the best result from the three feature vector fusion outperforms the best from the two feature vector fusion. As might be expected, when the feature vector is augmented with additional information about the target, the recognition rate is improved.

The proposed method was next applied to the data measured using the Michigan State University reflectivity arch scattering range, which is a bistatic measurement system. The measurement configuration is shown in Figure 11. Scattering targets were placed on a low density styrofoam column, which was positioned at the center of the arch, at the same height from the ground as the horn antennas to provide the most uniform incident field. Frequency-domain measured data were obtained for a frequency range of 2–5.81 GHz with a 30 MHz step increment, using an Agilent E5071C network analyzer. Aspect angles were varied from 0° to 30° relative to the nose, at 0.5° intervals. The bistatic angles between transmitter horn and receiver horn were set to 12.4°, 30° and 60°. (Note that 12.4° is

Table 2. Performance comparison of radar target recognition using three feature vector fusion (monostatic + two bistatic receivers) for calculated data.

Combination of Receivers	SNR [dB]				
	10	15	20	25	30
Mono + Bi30°	85.53	87.66	90.83	91.43	93.37
+ Bi60°	(2.36)	(1.36)	(0.89)	(0.90)	(0.57)
Mono + Bi30°	88.32	90.47	92.28	93.61	95.36
+ Bi90°	(2.20)	(1.28)	(0.69)	(0.63)	(0.29)
Mono + Bi30°	87.78	88.78	91.32	92.53	94.71
+ Bi120°	(1.92)	(1.45)	(1.29)	(0.73)	(0.49)
Mono + Bi30°	88.89	91.15	92.30	94.12	96.22
+ Bi150°	(2.12)	(1.10)	(1.06)	(0.55)	(0.49)
Mono + Bi60°	89.22	90.65	92.70	94.44	95.63
+ Bi90°	(1.91)	(1.06)	(0.57)	(0.78)	(0.36)
Mono + Bi60°	89.28	91.84	93.07	94.56	95.95
+ Bi120°	(1.60)	(1.14)	(0.61)	(0.81)	(0.35)
Mono + Bi60°	89.85	90.04	93.34	94.43	96.72
+ Bi150°	(2.03)	(1.17)	(0.68)	(0.55)	(0.55)
Mono + Bi90°	90.03	91.24	93.89	95.03	96.01
+ Bi120°	(1.95)	(1.17)	(1.03)	(0.67)	(0.47)
Mono + Bi90°	92.00	93.28	94.62	96.18	97.57
+ Bi150°	(1.88)	(0.96)	(0.85)	(0.63)	(0.39)
Mono + Bi120°	88.84	92.68	93.27	94.64	96.40
+ Bi150°	(1.85)	(0.90)	(0.81)	(0.91)	(0.49)

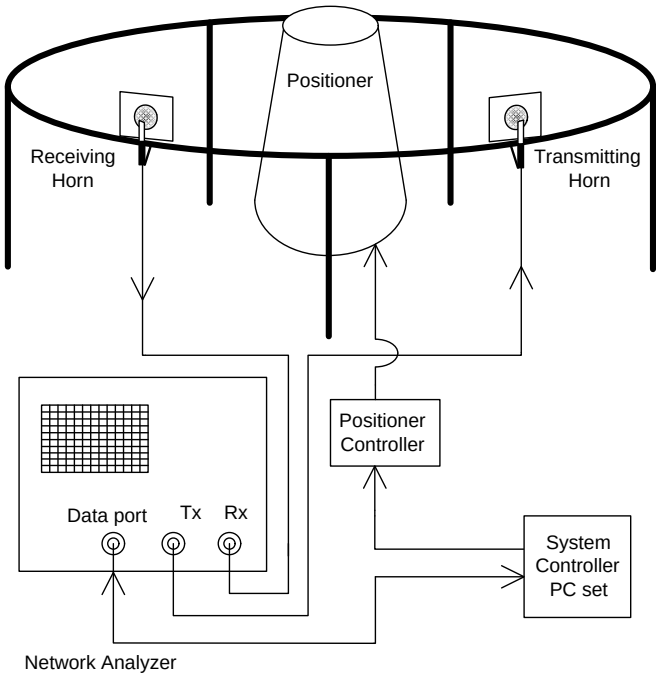

Figure 11. Bistatic radar measurement system at MSU.

Table 3. Performance comparison of radar target recognition using the feature vector fusion (monostatic + two bistatic receivers) for measured data.

Combination of Receivers	SNR [dB]				
	10	15	20	25	30
Mono + Bi12.4°	93.64	95.48	96.85	97.83	98.61
+ Bi30°	(1.31)	(0.93)	(0.11)	(0.46)	(0.40)
Mono + Bi12.4°	92.07	95.91	96.67	97.39	98.03
+ Bi60°	(1.57)	(1.08)	(0.91)	(0.61)	(0.59)
Mono + Bi30°	94.24	96.51	97.20	98.29	99.87
+ Bi60°	(1.40)	(1.08)	(0.76)	(0.37)	(0.22)

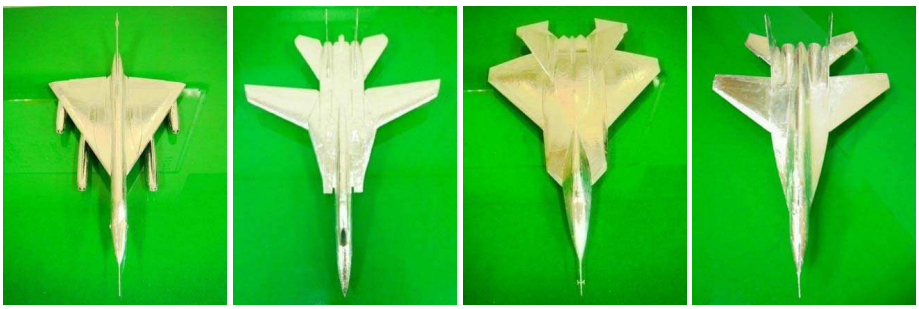

Figure 12. Scale model targets used for measurement, (a) B-58, (b) F-14, (c) F-22, and (d) Mig-29.

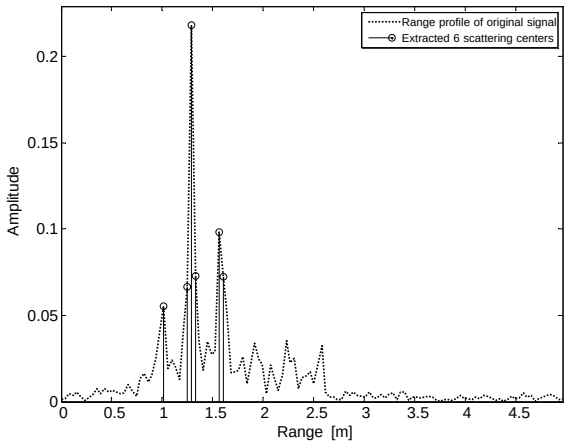

Figure 13. Extracted scattering centers from monostatic RCS of F-22 at aspect angle of 0°, SNR = 20 dB.

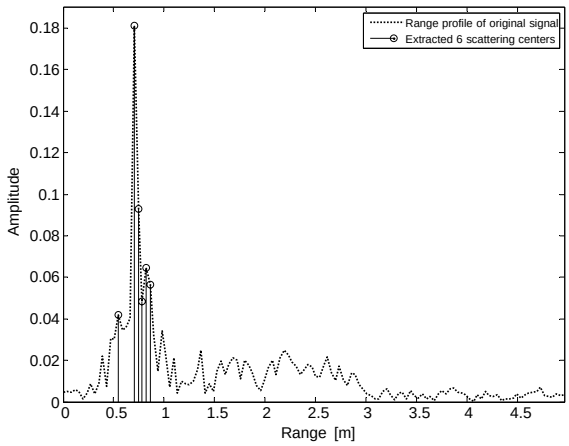

Figure 14. Extracted scattering centers from BRCS (bistatic angle = 30°) of F-22 at aspect angle of 0°, SNR = 20 dB.

the smallest bistatic angle allowed by the geometry of the measurement system). The four scale model targets (1 : 32 Mig-29, F-22, F-14 and 1 : 48 B-58) shown in Figure 12 were used for measurement.

Next the feature vectors for each target were extracted using FFT-based CLEAN. Figure 13 and Figure 14 show six extracted scattering centers for the F-22 scale model from the monostatic and bistatic angle = 30° at 0° aspect angle. The extracted 6 scattering centers (indicated as o) match well with the peaks of the range profile for the measured data, verifying that the FFT-based CLEAN works well

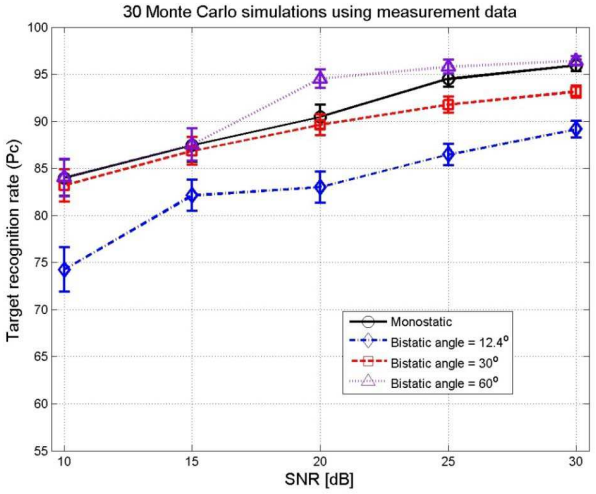

Figure 15. Performance comparison of radar target recognition using a single feature vector for measured data.

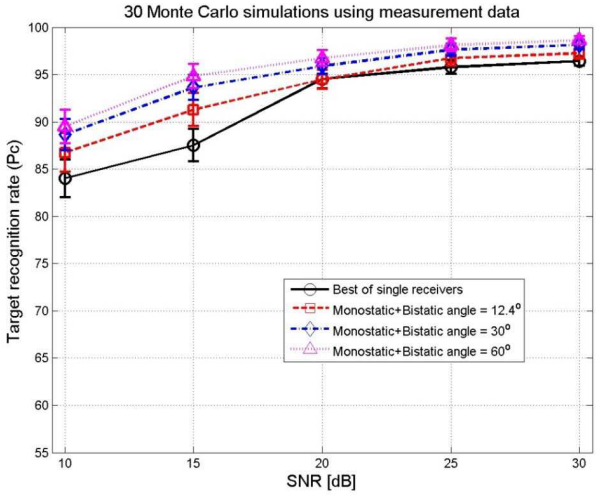

Figure 16. Performance comparison of radar target recognition using the feature vector fusion (monostatic + one bistatic receiver) for measured data.

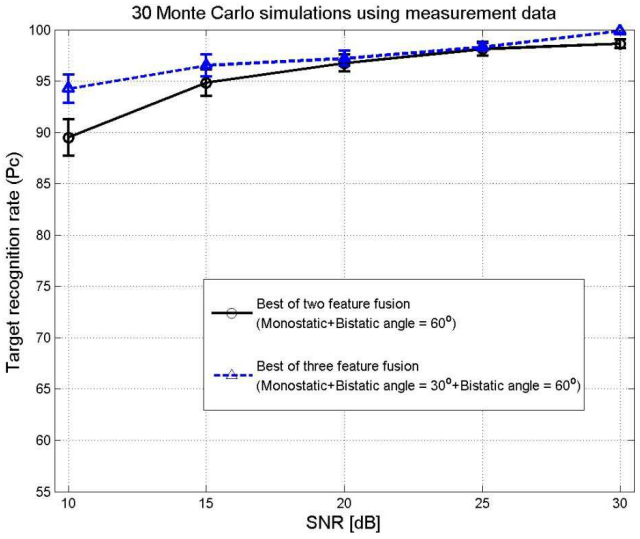

Figure 17. Performance comparison of radar target recognition for the best feature vector fusions of measured data.

for the measured data. The measured data are used for training and the noisy data created by adding white Gaussian noise at a given SNR are used for testing. At each monostatic and bistatic angles there are $4*61 = 244$ measured feature sets for training, and $4*61 = 244$ noisy feature sets for testing. Thirty Monte Carlo trials were used as in the computed data case.

As with the previous simulation using a calculated data, the target recognition rates were compared for three cases: (1) using a single receiver (2) using two receivers (monostatic and one bistatic) (3) using three receivers (monostatic and two bistatic). The results are shown in Figure 15, Figure 16 and Table 3. From Figure 15, it can be seen that the best target recognition rate using a single receiver occurs at the bistatic angle of 60° among the receiver positions. Figure 16 shows that all fusion feature sets of

two receivers were better than the best of the single receiver. From Table 3, we can see that the best performance of case (3) is found at the fusion of monostatic + bistatic angle = 30°+ bistatic angle = 60°. Figure 17 shows that the best of three feature vector fusion also outperforms the best of two feature vector fusion as with the results using computed data. Thus, the results using the measured data is consistent with the results from the calculated data.

4. CONCLUSION

This paper proposes a feature vector fusion technique for performance enhancement of radar target recognition. A study was done to compare the proposed technique to the existing method that does not use vector fusion. First, an experiment with three different CAD models of full-scale fighters was implemented based on RCS data calculated at the monostatic and bistatic angles of 30°, 60°, 90°, 120°, and 150°. Also, measured data from four scale-model targets at monostatic and bistatic angles of 12.4°, 30° and 60° were used for verification of the proposed method. The 1-D FFT-based CLEAN Algorithm was used to extract the scattering centers to use as the target feature vector. The extracted feature vector was used as input to a neural network classifier to conduct the target recognition experiment. It was determined that the target recognition performance was better with feature vector fusion than without, which validates the proposed method of enhanced target recognition performance. A future study is proposed to examine target recognition using feature vector fusion with only multiple bistatic receivers (two bistatic receivers or three bistatic receivers, but without monostatic data). Also it is important for future study to determine when the performance is saturated as the extent of feature vector fusion is increased (to determine the optimal feature vector fusion dimension).

ACKNOWLEDGMENT

This work was supported by the Basic Science Research Program through the National Research Foundation of Korea (NRF) funded by the Ministry of Education (No. NRF-2012R1A1A4A01009094).

REFERENCES

1. Choi, I.-S., "Extraction of scattering center and natural frequency using evolutionary programming-based CLEAN," Ph.D. Dissertation, POSTECH, 2003.
2. Seo, D.-K., K.-T. Kim, I.-S. Choi, and H.-T. Kim, "Wide-angle radar target recognition with subclass concept," *Progress In Electromagnetics Research*, Vol. 44, 231–248, 2004.
3. Cho, S.-W. and J.-H. Lee, "Effect of threshold value on the performance of natural frequency -based radar target recognition," *Progress In Electromagnetics Research*, Vol. 135, 527–562, 2013.
4. Kim, K.-T. and H.-T. Kim, "One-dimensional scattering centre extraction for efficient radar target classification," *IEE Proceedings — Radar, Sonar and Navigation*, Vol. 146, No. 3, 147–158, Jun. 1999.
5. Choi, I.-S., D.-K. Seo, J.-K. Bang, H.-T. Kim, and E. J. Rothwell, "Radar target recognition using one-dimensional evolutionary programming-based CLEAN," *Journal of Electromagnetic Waves and Applications*, Vol. 17, No. 5, 763–784, 2003.
6. Kim, K.-T., D.-K. Seo, and H.-T. Kim, "Radar target identification using one-dimensional scattering centres," *IEE Proceedings — Radar, Sonar and Navigation*, Vol. 148, No. 5, 285–296, Oct. 2001.
7. Li, X.-F., Y.-J. Xie, and R. Yang, "Bistatic RCS prediction for complex targets using modified current marching technique," *Progress In Electromagnetics Research*, Vol. 93, 13–28, 2009.
8. Alivizatos, E. G., M. N. Petsios, and N. K. Uzunoglu, "Towards a range-doppler UHF multistatic radar for the detection of non-cooperative targets with low RCS," *Journal of Electromagnetic Waves and Applications*, Vol. 19, No. 15, 2015–2031, 2005.
9. Wills, N. J., *Bistatic Radar*, 2nd Edition, SciTech Pub. Inc., 2007.
10. Willis, N. J. and H. D. Griffiths, *Advances in Bistatic Radar,* SciTech Pub. Inc., 2007.

11. Oraizi, H., A. Abdolali, and N. Vaseghi, "Application of double zero metamaterials as radar absorbing materials for the reduction of radar cross section," *Progress In Electromagnetics Research*, Vol. 101, 323–337, 2010.
12. Lee, S.-J. and I.-S. Choi, "Bistatic radar target classification using time-frequency analysis and multilayered perceptron neural network," *PIERS Proceedings*, 1569–1671, Marrakesh, Morocco, Mar. 20–23, 2011.
13. Radoi, E., A. Quinquis, and F. Totir, "Supervised self-organizing classification of super resolution ISAR images: An anechoic chamber experiment," *EURASIP Journal on Applied Signal Processing*, Vol. 2006, 1–14, 2006.
14. Taso, J. and R. D. Steinberg, "Reduction of sidelobe and speckle artifacts in microwave imaging: The CLEAN technique," *IEEE Transactions Antennas and Propagation*, Vol. 36, No. 4, 543–556, 1988.
15. Misiurewicz, J., K. S. Kulpa, Z. Czekala, and T. A. Filipek, "Radar detection of helicopters with application of CLEAN method," *IEEE Transactions Aerospace and Electronic Systems,* Vol. 48, No. 4, 3525–3537, 2012.
16. Hurst, M. P. and R. Mittra, "Scattering center analysis via Prony's method," *IEEE Transactions Antennas and Propagation*, Vol. 35, No. 8, 986–988, Aug. 1987.
17. Lee, J.-H., I.-S. Choi, and H.-T. Kim, "Natural frequency-based neural network approach to radar target recognition," *IEEE Transactions on Signal Processing*, Vol. 51, No. 12, 3191–3197, Dec. 2003.